COBEM 2021 26th International Congress of Mechanical Engineering
November 22-26, 2021, Virtual Congress, Brazil

Effect of segmented electrodes on piezoelectric energy harvesting performance from a graded metastructure

Camila Sanches Schimidt[1]
Vagner Candido de Sousa[2]
[1]Department of Aeronautical Engineering, Engineering School of São Carlos, University of São Paulo, São Carlos, SP 13566-590, Brazil
[2]Universidade Estadual Paulista (Unesp), Câmpus Experimental de São João da Boa Vista, São João da Boa Vista, SP, 13876-750, Brazil
camilaschimidt@usp.br
vagner.sousa@unesp.br

Carlos De Marqui Junior[1]
[1]Department of Aeronautical Engineering, Engineering School of São Carlos, University of São Paulo, São Carlos, SP 13566-590, Brazil
demarqui@sc.usp.br

Abstract. *This work investigates a piezoelectric energy harvesting from localized modes of a graded metamaterial beam (or metastructure). The metastructure has periodically distributed elastic resonators and the grading parameter is the linear variability in the resonant frequency of the elastic attachments. Moreover, the host beam is fully covered on the top and bottom surfaces by piezoceramic layers with continuous electrodes. A criterion for electrodes segmentation is presented to avoid cancellation of electrical output from a target localized mode. A load resistance is considered in the electrical domain of each electrode segment in order to estimate the power output. The governing equations are given using modal analysis, and the transverse displacement of the beam as well as power output from each segment are solved in the frequency domain. The electroelastic behaviors of a continuous electrode case and of a segmented electrode configuration are compared. The bandwidth increases 49% when an increasing linear variation in the frequency of the absorbers is considered. Furthermore, the power harvested for the segmented electrode configurations is orders of magnitude larger than that for the continuous electrodes configuration.*

Keywords: *Graded metastructure, energy harvesting, electrode configuration*

1. INTRODUCTION

Locally resonant metastructures, which were first reported in the seminal paper by Liu *et al.* (2000), have been an increasing focus by researchers due their ability to open low-frequency bandgaps (i.e., frequency bands where the waves are forbidden for wavelengths much longer than the lattice size). Although also widely investigated, bandgaps of phononic crystals (based on Bragg scattering) are generated at wavelengths comparable to the spatial scale of the periodicity and, therefore, are usually observed in high frequencies or require large structures to open at low-frequency range (Hussein *et al.* (2014); Lemoult *et al.* (2013)).

In order to enhance the vibration attenuation performance, researchers have investigated strategies to increase the bandwidth of locally resonant bandgaps: (i) centralize multiple bandgaps, as demonstrated by El-Borgi *et al.* (2020). (ii) combination of Bragg and LR bandgaps in a locally resonant beam (Xiao *et al.* (2012); Xiao *et al.* (2013)). (iii) the use of periodic arrays of shunted piezoelectric patches to control and widen the bandgap, in plates (Chen *et al.* (2013)) and rods (Thorp *et al.* (2001)). (iv) monostable and bistable nonlinear oscillators (Daqaq *et al.* (2014); Xia *et al.* (2019)), among others.

A new class of locally resonant metastructure, a graded matastructure, has increased the attention of researchers due to their enhanced wave manipulation capabilities, producing phenomena such as, increasing bandgap width, energy localization and wave trapping. Different from the commonly locally resonant metamaterials, where identical resonators are periodically distributed along a host structures, the graded metastructure are obtained from a smooth variation of a particular parameter (grading parameter) of the resonators. The physical effects of the variability on the wave propagation of metamaterial beams were discussed by Beli *et al.* (2019). The same authors also discussed the behavior of a rainbow metamaterial with spatially correlated linear variation of the Young's modulus of the equally spaced resonators. The experimental wave attenuation capabilities due to a random array of eighteen PZT patches in a aluminum beam were presented by Cardella *et al.* (2016). The use of spectral element method (SEM) to model a graded metamaterial, with local resonators with the same mass but different natural frequencies, is presented by Hu *et al.* (2021).

The reduction in electrical power consumption of systems, such as sensor nodes, has motivated the research on vibration energy harvesting. Among the available vibration-to-electric energy conversion mechanisms are the electromagnetic one, (Williams and Yates (1996); Glynne-Jones *et al.* (2004); Arnold (2007)), the electrostatic (Roundy *et al.* (2004); Mitcheson *et al.* (2004)), magnetostriction (Wang and Yuan (2008); Adly *et al.* (2010)) and piezoelectric (Roundy *et al.* (2003); Jeon *et al.* (2005)). The piezoelectric materials have attracted significant research interest due their large power density and ease of application (Erturk and Inman (2011)). Due to the ability to localize energy in space, graded matamaterials have received considerable attention to increase the energy harvesting efficiency. A graded array of resonant rods attached to an elastic beam for enhanced energy harvesting capability was presented in studies by Ponti *et al.* (2020a,b). Numerical results obtained from a piezoelectric bimorph cantilever presented by Alshaqaq and Erturk (2020) demonstrated the enhanced vibration attenuation bandwidth, the localization of vibration, and the harvested power of a graded locally resonant metamaterial beam obtained through the variation of the resonant frequency of the resonant piezoelectric unit cells.

In the present work, an electromechanically coupled Euler-Bernoulli beam with periodically distributed elastic resonators, and the grading parameter is the linear variation of their resonances, is investigated for piezoelectric energy harvesting from localized modes. First, the piezoelectric energy harvesting performance is discussed for continuous electrodes of the piezoelectric layers. Later, a segmented electrode configurations is exploited to avoid cancellation of electrical output. The electrical power output of the segmented case is orders of magnitude larger than the continuous one. In Section 2, we present the theoretical background of the bimorph piezoelectric beam. The equations of motion are summarized from modal analysis. In Section 3, the effects of the grading parameter on the vibration suppression and energy harvesting are demonstrated for the continuous and segmented electrodes configurations. In the end, the conclusions are presented.

2. THEORETICAL BACKGROUND

Consider a cantilever bimorph piezoelectric beam with mechanical resonators evenly distributed and under harmonic base excitation, as shown in figure 1. The electrodes are segmented as pairs and connected to a total of S parallel shunt circuits with voltage $v_j(t)$ between the jth pair of electrodes, where x_j^L and x_j^R are the left and right ends of the electrodes and Δx_j is the length of each electrode. The spring-mass absorbers attached to the beam are modeled as single degree of freedom systems, and each resonator has mass m_f and stiffness k_f, located at a position x_f, and the total number of resonators is denoted by P. In the present work, the frequencies of the absorbers (grading parameter) follows a linear variation, as will be later discussed. Using Euler-Bernoulli theory Sugino *et al.* (2018) the governing equations are given by

$$EI\frac{\partial^4 w}{\partial x^4} + m\frac{\partial^2 w}{\partial t^2} - \sum_{f=1}^{P} k_f u_f(t)\delta(x - x_f) - \theta\sum_{j=1}^{S} v_j(t)\frac{\partial^2}{\partial x^2}\left[H(x - x_j^L) - H(x - x_j^R)\right] = m\frac{d^2 w_b}{dt^2} \tag{1}$$

$$m_f\frac{d^2 u_f}{dt^2} + k_f u_f(t) + m_f\frac{d^2 w(x_f, t)}{dt^2} = -m\ddot{w}_b \tag{2}$$

$$C_{p,j}\frac{dv_j}{dt} + Y_j v_j(t) + \theta\int_{x_j^L}^{x_j^R}\frac{\partial^3 w}{\partial x^2 \partial t} = 0 \tag{3}$$

where $w(x,t)$ is the transverse displacement of the beam, $u_f(t)$ is the displacement of the fth resonator, Y_j the admittance across the jth electrode pair, $H(x)$ is the Heaviside function,

The piezoelectric layers and the substructure have the same width, b, while h_s and ρ_s are the thickness and density of the structure, respectively. The piezoelectric layers have mass density ρ_p, thickness h_p, elastic modulus at constant electric field $\bar{c}_{11}^E$, effective piezoelectric stress constant $\bar{e}^{31}$, and permittivity component at constant strain $\bar{\varepsilon}_{33}^T$. The total mass m and flexural stiffness (EI) of the composite cross section are, respectively given by,

$$m = b(\rho_s h_s + 2\rho_p h_p) \tag{4}$$

$$EI = \frac{2b}{3}\left[c_s\frac{h_s^3}{8} + \bar{c}_{11}^E\left(\left(h_p + \frac{h_s}{2}\right)^3 - \frac{h_s^3}{8}\right)\right] \tag{5}$$

and θ is the electromechanical coupling term and $C_{p,j}$ is the piezoelectric capacitance across the jth electrode pair, defined as,

$$\theta = \bar{e}_{31} b(h_s + h_p) \tag{6}$$

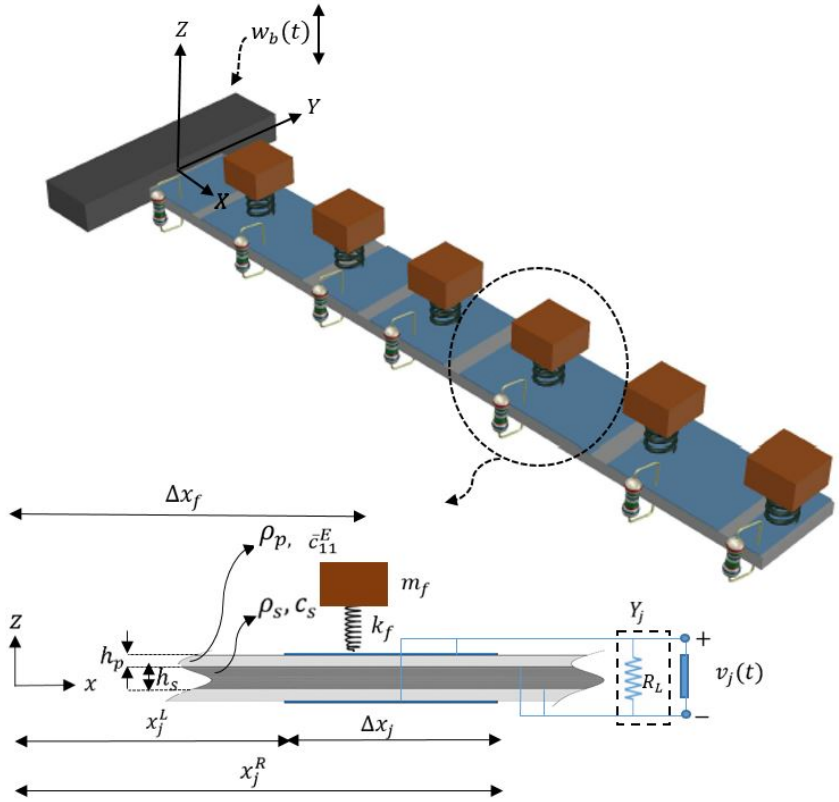

Figure 1: Schematic of the combined mechanical metastructure with piezoelectric layers under harmonic base excitation for segmented electrodes with different lengths.

$$C_{p,j} = \frac{2\bar{\varepsilon}_{33}^s}{h_p}\Delta x_j \tag{7}$$

The properties of the piezoelectric layers are reduced from $3D$ constitutive equations, where the overbars indicate effective properties for $1D$ thin layers.

$$\bar{c}_{11}^E = \frac{1}{s_{11}^E}, \quad \bar{e}^{31} = \frac{d_{31}}{s_{11}^E}, \quad \bar{\varepsilon}_{33}^s = \bar{\varepsilon}_{33}^T - \frac{d_{31}^2}{s_{11}^E} \tag{8}$$

where s_{11}^E is the elastic compliance at constant electric field, d_{31} is the piezoelectric strain constant, $\bar{\varepsilon}_{33}^T$ is the permittivity component at constant stress.

Assuming that the transverse vibration of the beam may be represented in terms of a finite number of modes N, which is expressed by,

$$w(x,t) = \sum_{r=1}^{N} \phi_r(x)\eta_r(t) \tag{9}$$

where $\phi_r(x)$ are the undamped short-circuit modes of vibration and $\eta_r(t)$ are the modal coordinates. Assuming ω_r as the rth natural frequency of the plain structure at short circuit, the mass-normalized mode shapes are normalized as,

$$\int_0^L m\phi_r(x)\phi_s(x)dx = \delta_{rs}, \qquad \int_0^L EI\phi_r(x)\frac{d^4\phi_r(x)}{dx^4}dx = \omega_r^2\delta_{rs} \qquad r,s = 1,2... \tag{10}$$

where δ_{rs} is the Kronecker delta. Substituting equation (9), into the governing equations (1-3), and applying the orthogonality condition (see Meirovitch (1997) for more details), we can obtain the expressions in modal coordinates as follow,

$$\ddot{\eta}_r(t) + \omega_r^2\eta_r(t) + \sum_{f=1}^{P} m_f\phi_r(x_f)\sum_{k=1}^{N}\ddot{\eta}_k(t)\phi_k(x_f) + \sum_{f=1}^{P} m_f\ddot{u}_f\phi_r(x_f) - \theta\sum_{j=1}^{S} v_j(t)\Delta\phi_{r,j}^{'} = q_r(t) \tag{11}$$

$$m_f\ddot{u}_f(t) + k_f u_f(t) + m_f\sum_{k=1}^{N}\ddot{\eta}_k(t)\phi_k(x_f) = -m\frac{d^2w_b}{dt^2} \tag{12}$$

$$C_{p,j}\dot{v}_j(t) + Y_J[v_j(t)] + \theta \sum_{r=1}^{N} \dot{\eta}_r(t)\Delta\phi_{r,j}^{'} = 0 \tag{13}$$

The modal forcing due to arbitrary base motion is given by,

$$q_r(t) = -m\frac{d^2 w_b}{dt^2}\left(\int_0^L \phi_k(x)dx + \sum_{f=1}^{P} m_f \phi_k(x_f)\right) \tag{14}$$

and $\Delta\phi_{k,j}^{'}$ is a slope difference defined as

$$\Delta\phi_{k,j}^{'} = \left(\frac{d\phi_r}{dx}\right)_{x_j^L}^{x_j^R} = \frac{d\phi_r(x_j^R)}{dx} - \frac{d\phi_r(x_j^L)}{dx} \tag{15}$$

Assuming that the response of the system is harmonic at some excitation frequency ω, we can determine the absorbers and voltage amplitudes as,

$$\overline{u}_f = \frac{\overline{w}_b\omega^2}{\omega_t^2 - \omega^2} + \frac{\omega^2}{\omega_t^2 - \omega^2}\sum_{k=1}^{N}\overline{\eta}_k\phi_k(x_f) \tag{16}$$

$$\overline{v}_j = \frac{-i\omega\theta\sum_{k=1}^{N}\overline{\eta}_k\Delta\phi_{r,j}^{'}}{-i\omega C_{p,j} + Y_j} \tag{17}$$

Substituting into equation (11),

$$\left(\omega_r^2 - \omega^2\right)\overline{\eta}_r - \omega^2\sum_{k=1}^{N}\sum_{f=1}^{P}\frac{\hat{m}_f\omega_t^2}{\omega_t^2 - \omega^2}\phi_k(x_f)\phi_r(x_f)\overline{\eta}_k + \frac{\alpha i\omega}{i\omega + h(i\omega)}\sum_{k=1}^{N}\sum_{j=1}^{S} EI\frac{\Delta\phi_{k,j}^{'}}{\Delta x_j}\frac{\Delta\phi_{r,j}^{'}}{\Delta x_j}\Delta x_j\Delta x_j\overline{\eta}_k = \overline{Q}_r \tag{18}$$

where $\hat{m}_f$ is the normalized mass of jth absorber $m_f/(mL)$, $\omega_t = \sqrt{(k_f/m_f)}$ is the absorber's natural frequency and α is a dimensionless parameter Sugino *et al.* (2017) related to electromechanical coupling, flexural stiffness, and piezoelectric capacitance, given by,

$$\alpha = \frac{\theta^2}{EI\hat{C}_p} \tag{19}$$

where $\hat{C}_p$ is the effective piezoelectric capacitance per electrode length, and $h(\omega) = Y_j(\omega)/C_{p,j}$ is the normalized admittance. In the present work, we consider a resistive energy harvesting circuit as $Y_j = 1/R_L$.

In this study, the elastic absorbers can be tuned to a single target frequency or graded. Therefore, the target frequencies of the resonant attachments follow the linear law,

$$\omega_t(n) = \omega_k\left(1 + \beta\left(n\Delta - \frac{L}{2}\right)\right) \tag{20}$$

where ω_k is a natural frequency of the plain beam, n is the unit cell, the slope of disorder degree is β ($0 \leq \beta \leq 1$), and Δ is the distance between resonators. The limits of the bandgap of elastic metamaterials made from locally resonant arrays are determined by Sugino *et al.* (2016),

$$\omega_t < \omega < \omega_t\sqrt{1+\mu} \tag{21}$$

where, $\mu = \sum_{f=1}^{P}\hat{m}_f$. This closed form is derived using the infinite resonator approximation and can not be used to predict the bandgap limits of graded metamaterials. Therefore, we use the approach presented in Celli *et al.* (2019); Alshaqaq and Erturk (2020), to determine when we achieve a bandgap. In this work, we can define the transmissibility as the ratio of displacement at a given point of the beam (x) to the base displacement,

$$|TR(\omega)| = \left|\frac{w_{abs}(x)}{w_b}\right| \tag{22}$$

3. RESULTS

We consider a cantilever bimorph beam made from aluminum substructure, with length $L = 900$ mm, thickness $h_s = 0.8$ mm, density $\rho_s = 2700$ kg/m^3, and elastic modulus $c_s = 69$ GPa. The host beam is covered on the top and bottom surfaces by piezoceramic layers of PZT-5A. The length and the thickness of the PZT layers are the same of the host beam. The density, elastic modulus, effective piezoelectric stress constant, and the permittivity component at constant strain are, respectively, $\rho_p = 7750$ kg/m^3, $\bar{c}_{11}^E = 61$ GPa, $\bar{e}_{31} = -10.4$ C·m^{-2} and $\bar{\varepsilon}_{33}^S = 13.3$ nF·m^{-1}.

A total of 20 elastic damped resonators are uniformly distributed along the plain electromechanical beam. Besides the small damping considered in the absorbers ($\zeta_f = 0.001$), a modal damping ratio is considered as follow,

$$\zeta_k = \frac{A}{2\omega_k} + \frac{B\omega_k}{2} \tag{23}$$

where $A = 1$ and $B = 0$.

3.1 Effect of variability in absorbers on vibration attenuation

Figure (2) displays the transmissibility heatmaps as function of normalized excitation and variability (β). Ascending and descending patterns for the frequency of the resonators are considered, *i.e.*, positive and negative β values, respectively. We observe the following from the figure: (i) the bandgap bandwidth increases with increasing the variability (*i.e.*, absolute β value), (ii) positive β values exhibit fewer bandgaps than negative β values, (iii) for high absolute β values, individual bandgaps are created, which produces vibration peaks between the individual attenuation zones.

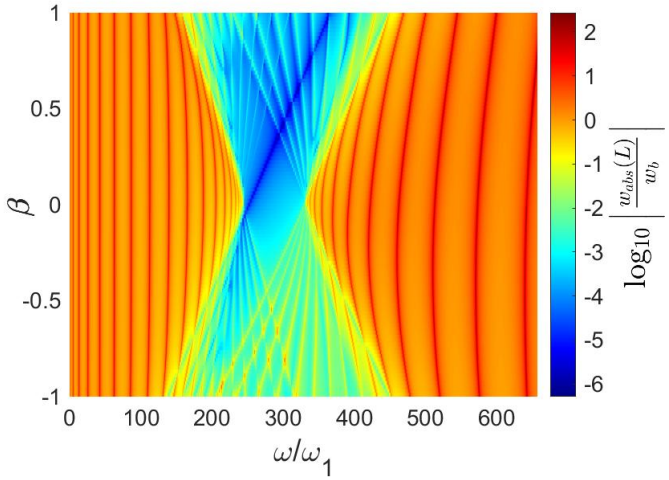

Figure 2: Transmissibility heatmaps versus frequency grading patterns and normalized excitation frequency.

The differences for the ascending and descending frequency of the absorbers in the bandgap formation are presented in figure (3), that displays the tip transmissibility versus normalized excitation frequency. To compare the effect of the variability in the bandgap, we analyze three cases, the uniform one, when $\beta = 0$ (red line), and two cases considering a disorder in the target frequency of the absorbers, with equal absolute values, $\beta = 0.526$ (blue and orange lines). The approach presented by Celli *et al.* (2019); Alshaqaq and Erturk (2020) is considered to make the comparison, where we assume that we achieve a bandgap when $|TR|(\omega) \leq 0.1$, which is represented by the dashed black line. From the figure, it is possible to see that a mistuning in the frequencies increases the attenuation bandwidth, and the intensity of the attenuation decreases. We can observe that the positive β value produces a stronger attenuation intensity inside the bandgap region, when compared to the negative value.

Figure (4) presents the transmissibility as a function of space and normalized frequency for an elastic metamaterial, for three cases. The first is considering a linear descending mistuning in frequency of the absorbers (4a). From the figure, is possible to see a wave trapping region (*i.e.*, linear wave trapping-attenuation interface in space). As the normalized frequency increases, the mode localization slowly move from the tip of the beam toward the clamped end. When a uniform case is adopted, *i.e.*, all the absorbers are tuned at the same frequency, a uniform bandgap is observed from the clamped to the free end of the metastructure (4b). Different from pattern presented by negative β values, for positive β values (*i.e.*, ascending pattern in the frequency of the resonators), as the normalized frequency increases, the bandgap varies along the frequency and metastructure length (bandgap broadening vibration) from clamped end toward the tip of the beam.

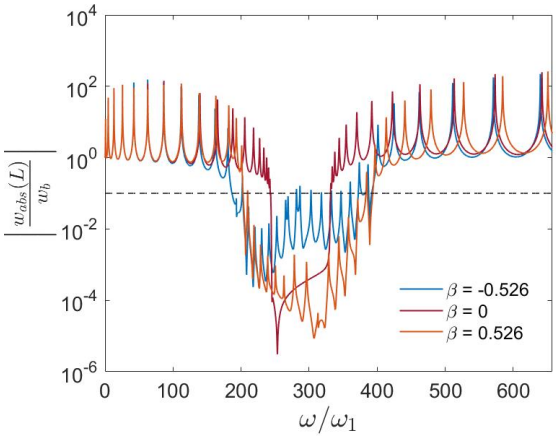

Figure 3: Tip transmissibility versus normalized excitation frequency, $R_L = 100\Omega$ is considered.

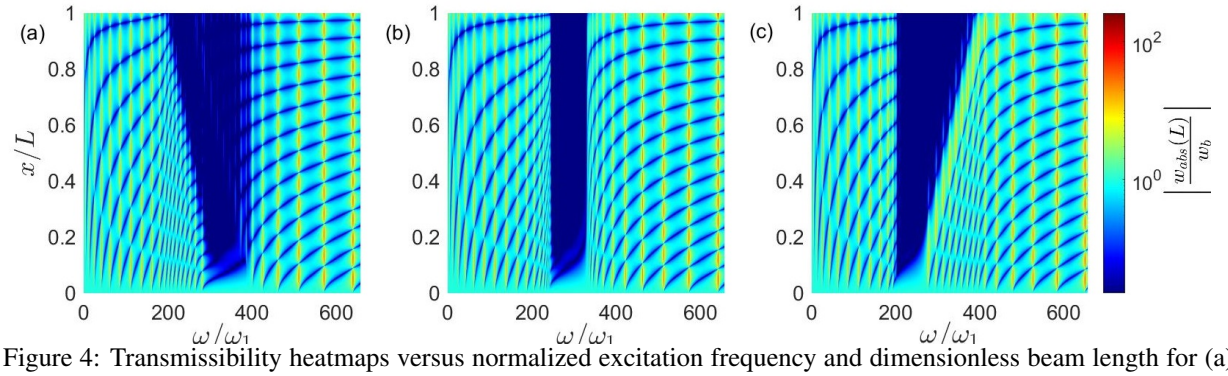

Figure 4: Transmissibility heatmaps versus normalized excitation frequency and dimensionless beam length for (a) considering a descending mistuning in frequencies of the absorbers, $\beta = -0.526$, (b) uniform case, $\beta = 0$ and (b) considering an ascending mistuning in frequencies of the absorbers, $\beta = 0.526$. $R_L = 100\Omega$ and $\zeta_f = 0.0001$ are considered.

3.2 Energy harvesting in a graded metamaterial with continuous electrodes

When an ascending mistuning in the frequency of the absorber is considered, *i.e.*, $\beta > 0$, the frequency range where wave trapping occurs as the frequency increases the percentage of energy located along the beam length increases, as is possible to see in figure (5). Figure (5a) presents the highest attenuation zone, approximately 70% of the beam length, for $\omega/\omega_1 = 278.22$. As the normalized frequency increases, the attenuation zone decreases. Figures (5b) and (5c) present approximately 40% and 30% of beam length with attenuation region, respectively. When the normalized frequency considered is $\omega/\omega_1 = 371.44$, energy is located in almost 80% of the beam length (figure 5d).

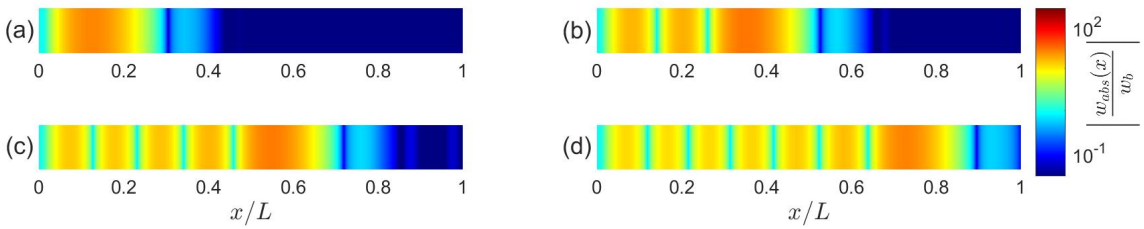

Figure 5: Transmissibility heatmaps versus dimensionless beam length, considering an ascending pattern in frequency of the resonators ($\beta = 0.562$), for (a) $\omega/\omega_1 = 278.22$, (b) $\omega/\omega_1 = 313.06$, (c) $\omega/\omega_1 = 343.56$ and (d) $\omega/\omega_1 = 371.44$. $\beta = 0.526$ and $R_L = 100\Omega$ are considered

Energy can be harvested from the region where mechanical energy is concentrated. For example, the power output is analyzed for a frequency $\omega/\omega_1 = 343.5$, for a set of load resistances that ranges from a short circuit condition (small values) to open circuit condition (high values), considering continuous electrodes. From the figure 6, we can notice that as the resistive load increases, the power increases until the optimum resistive load (for maximum power output) of 500Ω is achieved. For resistive loads higher than 500Ω, the electrical power output decreases.

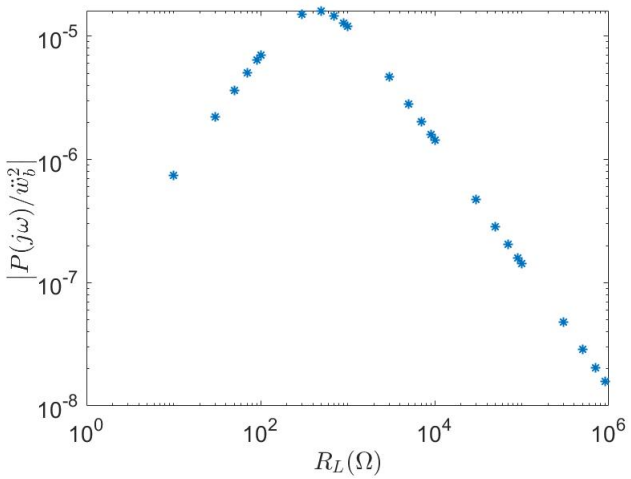

Figure 6: Power FRF versus resistive load, using continuous electrodes for $\omega/\omega_1 = 313.06$ and $\beta = 0.526$.

3.3 Energy harvesting in graded metamaterial with segmented electrodes

The literature that modes other than the fundamental one have strain nodes in a cantilever beam (Erturk *et al.* (2009)). Strain nodes are points where the strain distribution changes sign. Therefore, covering strain nodes with continuous electrodes results in the reduction of energy harvested due to the cancellation of the electrical output (or reduced electromechanical coupling). Therefore, a segmented electrodes configuration is considered for enhanced piezoelectric energy harvesting performance from the localized mode considered in the previous section ($\omega/\omega_1 = 313.06$).

The curvature of this localized mode is presented in figure (7). The curvature is defined as the product of the second derivative of the modal matrix ($\phi_k^{''}(x)$) and the modal displacement (η_k). A point of segmentation is assumed when $\phi_k^{''}(x)\eta_k = 0$ in figure (7). From this criterion, the electrodes are segmented in five regions as displayed in the figure, each one connected to a load resistance for electrical power output estimation. The power output against the load resistance of segments I to IV is presented in figure 8.

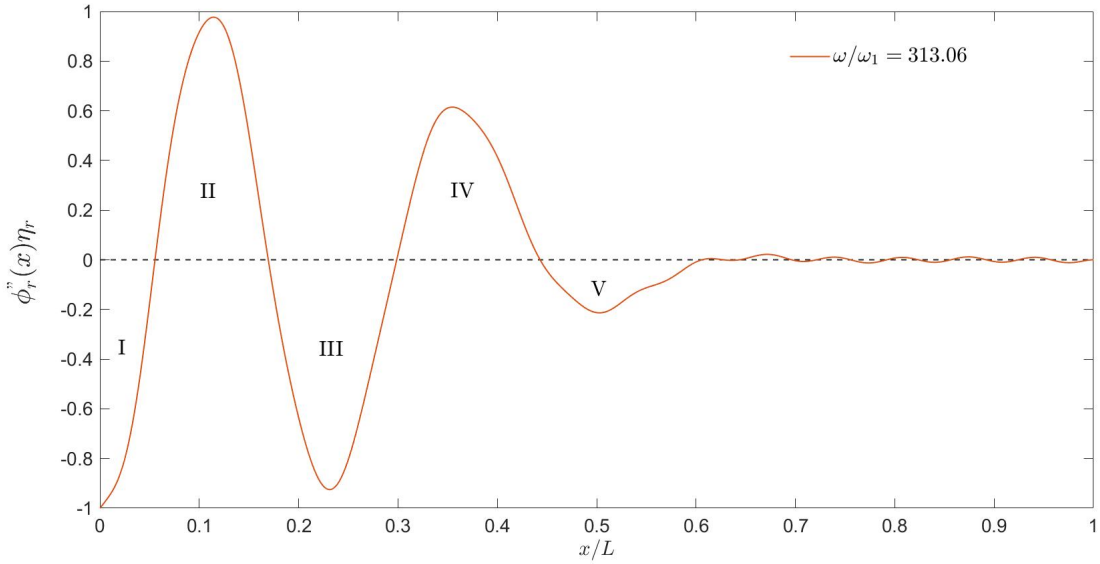

Figure 7: Normalized curvature $\phi_k^{''}(x)\eta_k$ at $\omega/\omega_1 = 313.06$ considering a mistuning in frequencies of the absorbers. $\beta = 0.526$ and $R_L = 100\ \Omega$ are considered.

The maximum power output from the target localized mode ($\omega/\omega_1 = 313.06$) is from the third segment, which is approximately $10.55\ \mu W/\ddot{w}_b^2$ for a load resistance of $R_L = 3K\Omega$. Table 1 presents maximum power output (considering the optimum load) from the continuous configuration and also from each segment of the segmented configuration. The power output from each segment is orders of magnitude larger than that from the continuous one, showing that the segmented configuration avoids the cancellation of electrical output observed in the continuous case.

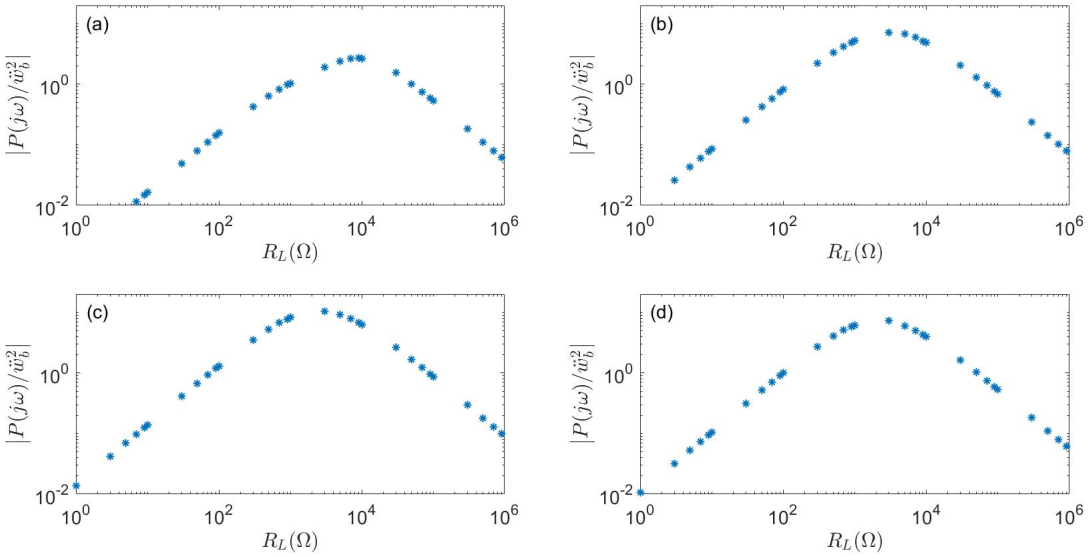

Figure 8: Power FRF versus resistive load, for (a) first segment, (b) second segment, (c) third segment and (d) fourth segment. $\omega/\omega_1 = 313.06$ and $\beta = 0.526$ are considered.

	$\lvert P(j\omega)/w_b^2 \rvert$	$R_L(\Omega)$
Continuous electrodes	$1.61{\cdot}10^{-5}$	500
1^o segment	2.70	9000
2^o segment	7.23	3000
3^o segment	10.55	3000
4^o segment	7.26	3000
5^o segment	0.93	3000

Table 1: Power output for continuous and segmented electrodes, considering $\omega/\omega_1 = 313.06$ and $\beta = 0.526$.

4. CONCLUSIONS

In this work, a cantilever bimorph piezoelectric beam with mechanical resonators was considered. The governing equations were presented and the transverse displacement of the beam as well as electrical power output were solved in the frequency domain. A linear variability in the frequency of mechanical resonators, around ω_{10} was considered, to obtain a graded matastructure. The ascending and descending variation of the frequency of the mechanical attachments increases the attenuation bandwidth while and the intensity decreases, when compared with the uniform case. For the studied cases, if high β values are considered, individual bandgaps are created, which produces vibration peaks between the individuals attenuation zones. Piezoelectric energy harvesting from a localized modes was analyzed for continuous and segmented electrodes configurations. The criteria for electrodes configuration was based on strain nodes of the host surface. Covering the strain nodes results in reduced electromechanical coupling and, therefore, electrical output cancellation. Therefore, for the localized mode discussed in this work, the electrical power output from the segmented electrode configuration is orders of magnitude larger than that from the continuous electrodes case.

5. REFERENCES

Adly, A., Davino, D., Giustiniani, A. and Visone, C., 2010. "Experimental tests of a magnetostrictive energy harvesting device and its modeling". *Journal of Applied Physics - J APPL PHYS*, Vol. 107. doi:10.1063/1.3357403.

Alshaqaq, M. and Erturk, A., 2020. "Graded multifunctional piezoelectric metastructures for wideband vibration attenuation and energy harvesting". *Smart Materials and Structures*, Vol. 30, No. 1, p. 015029. doi:10.1088/1361-665x/abc7fa.

Arnold, D.P., 2007. "Review of microscale magnetic power generation". *IEEE Transactions on Magnetics*, Vol. 43, No. 11, pp. 3940–3951. doi:10.1109/TMAG.2007.906150.

Beli, D., Fabro, A.T., Ruzzene, M. and Arruda, J.R.F., 2019. "Wave attenuation and trapping in 3d printed cantilever-in-mass metamaterials with spatially correlated variability". *Scientific Reports*, Vol. 9, p. 5617. doi:10.1038/s41598-019-41999-0.

Cardella, D., Celli, P. and Gonella, S., 2016. "Manipulating waves by distilling frequencies: a tunable shunt-enabled rainbow trap". *Smart Materials and Structures*, Vol. 25, No. 8, p. 085017. doi:10.1088/0964-1726/25/8/085017. URL https://doi.org/10.1088/0964-1726/25/8/085017.

Celli, P., Yousefzadeh, B., Daraio, C. and Gonella, S., 2019. "Bandgap widening by disorder in rainbow metamaterials". *Applied Physics Letters*, Vol. 114. doi:10.1063/1.5081916.

Chen, S., Wang, G., Wen, J. and Wen, X., 2013. "Wave propagation and attenuation in plates with periodic arrays of shunted piezo-patches". *Journal of Sound and Vibration*, Vol. 332, No. 6, pp. 1520–1532. ISSN 0022-460X. doi: https://doi.org/10.1016/j.jsv.2012.11.005.

Daqaq, M.F., Masana, R., Erturk, A. and Dane Quinn, D., 2014. "On the Role of Nonlinearities in Vibratory Energy Harvesting: A Critical Review and Discussion". *Applied Mechanics Reviews*, Vol. 66, No. 4. ISSN 0003-6900. doi:10.1115/1.4026278. URL https://doi.org/10.1115/1.4026278. 040801.

El-Borgi, S., Fernandes, R., Rajendran, P., Yazbeck, R., Boyd, J. and Lagoudas, D., 2020. "Multiple bandgap formation in a locally resonant linear metamaterial beam: Theory and experiments". *Journal of Sound and Vibration*, Vol. 488, p. 115647. ISSN 0022-460X. doi:https://doi.org/10.1016/j.jsv.2020.115647.

Erturk, A. and Inman, D., 2011. *Piezoelectric Energy Harvesting*. Wiley.

Erturk, A., Tarazaga, P.A., Farmer, J.R. and Inman, D.J., 2009. "Effect of strain nodes and electrode configuration on piezoelectric energy harvesting from cantilevered beams". *J. Vib. Acoust*, Vol. 131. doi:10.1115/1.2981094.

Glynne-Jones, P., Tudor, M., Beeby, S. and White, N., 2004. "An electromagnetic, vibration-powered generator for intelligent sensor systems". *Sensors and Actuators A: Physical*, Vol. 110, No. 1-3, pp. 344–349.

Hu, G., C. M. Austin, A., Sorokin, V. and Tang, L., 2021. "Metamaterial beam with graded local resonators for broadband vibration suppression". *Mechanical Systems and Signal Processing*, Vol. 146, p. 106982. ISSN 0888-3270. doi: https://doi.org/10.1016/j.ymssp.2020.106982.

Hussein, M.I., Leamy, M.J. and Ruzzene, M., 2014. "Dynamics of phononic materials and structures: Historical origins, recent progress, and future outlook". *Applied Mechanics Reviews*, p. 040802. doi:https://doi.org/10.1115/1.4026911.

Jeon, Y., Sood, R., h. Jeong, J. and Kim, S.G., 2005. "Mems power generator with transverse mode thin film pzt". *Sensors and Actuators A: Physical*, Vol. 122, No. 1, pp. 16–22. ISSN 0924-4247. doi: https://doi.org/10.1016/j.sna.2004.12.032. SSSAMW 04.

Lemoult, F., Kaina, N., Fink, M. and Lerosey, G., 2013. "Wave propagation control at the deep subwavelength scale in metamaterials". *Nature Physics*, Vol. 9. doi:10.1038/nphys2480.

Liu, Z., Zhang, X., Mao, Y., Zhu, Y.Y., Yang, Z., Chan, C.T. and Sheng, P., 2000. "Locally resonant sonic materials". *Science*, Vol. 289, No. 5485, pp. 1734–1736. ISSN 0036-8075. doi:10.1126/science.289.5485.1734.

Meirovitch, L., 1997. *Principles and Techniques of Vibrations*. Prentice-Hall, Inc., Upper Saddle River, NJ.

Mitcheson, P., Miao, P., Stark, B., Yeatman, E., Holmes, A. and Green, T., 2004. "Mems electrostatic micropower generator for low frequency operation". *Sensors and Actuators A*, Vol. 115, pp. 523–529. doi:10.1016/j.sna.2004.04.026.

Ponti, J.M.D., Colombi, A., Riva, E., Ardito, R., Braghin, F., Corigliano, A. and Craster, R.V., 2020a. "Experimental investigation of amplification, via a mechanical delay-line, in a rainbow based metamaterial for energy harvesting". *Applied Physics Letters*, Vol. 117. doi:https://doi.org/10.1063/5.0023544.

Ponti, J.M.D., Colombi, A., Ardito, R., Braghin, F., Corigliano, A. and Craster, R.V., 2020b. "Graded elastic metasurface for enhanced energy harvesting". *New Journal of Physics*, Vol. 22, No. 1, p. 013013. doi:10.1088/1367-2630/ab6062. URL https://doi.org/10.1088/1367-2630/ab6062.

Roundy, S., Wright, P.K. and Rabaey, J., 2003. "A study of low level vibrations as a power source for wireless sensor nodes". *Computer Communications*, Vol. 26, No. 11, pp. 1131–1144. ISSN 0140-3664. doi: https://doi.org/10.1016/S0140-3664(02)00248-7. Ubiquitous Computing.

Roundy, S., Wright, P.K. and Rabaey, J.M., 2004. *Energy Scavenging for Wireless Sensor Networks*. Springer US.

Sugino, C., Leadenham, S., Ruzzene, M. and Erturk, A., 2017. "An investigation of electroelastic bandgap formation in locally resonant piezoelectric metastructures". *Smart Materials and Structures*, Vol. 26, No. 5, p. 055029. doi: 10.1088/1361-665x/aa6671.

Sugino, C., Ruzzene, M. and Erturk, A., 2018. "Merging mechanical and electromechanical bandgaps in locally resonant metamaterials and metastructures". *Journal of the Mechanics and Physics of Solids*, Vol. 116, pp. 323–333. ISSN 0022-5096. doi:https://doi.org/10.1016/j.jmps.2018.04.005.

Sugino, C., Leadenham, S., Ruzzene, M. and Erturk, A., 2016. "On the mechanism of bandgap formation in locally resonant finite elastic metamaterials". *J. Appl. Phys.* doi:10.1063/1.4963648.

Thorp, O., Ruzzene, M. and Baz, A., 2001. "Attenuation and localization of wave propagation in rods with periodic shunted piezoelectric patches". *Smart Materials and Structures*, Vol. 10, No. 5, pp. 979–989. doi:10.1088/0964-1726/10/5/314.

Wang, L. and Yuan, F.G., 2008. "Vibration energy harvesting by magnetostrictive material". *Smart Materials and Structures*, Vol. 17, pp. 45009–14. doi:10.1088/0964-1726/17/4/045009.

Williams, C. and Yates, R., 1996. "Analysis of a micro-electric generator for microsystems". *Sensors and Actuators A:*

Physical, Vol. 52, No. 1, pp. 8–11. ISSN 0924-4247. doi:https://doi.org/10.1016/0924-4247(96)80118-X. Proceedings of the 8th International Conference on Solid-State Sensors and Actuators Eurosensors IX.

Xia, Y., Ruzzene, M. and Erturk, A., 2019. "Dramatic bandwidth enhancement in nonlinear metastructures via bistable attachments". *Applied Physics Letters*, Vol. 114, No. 9, p. 093501. doi:10.1063/1.5066329. URL `https://doi.org/10.1063/1.5066329`.

Xiao, Y., Wen, J. and Wen, X., 2012. "Broadband locally resonant beams containing multiple periodic arrays of attached resonators". *Physics Letters A*, Vol. 376, No. 16, pp. 1384–1390. doi:10.1016/j.physleta.2012.02.059.

Xiao, Y., Wen, J., Yu, D. and Wen, X., 2013. "Flexural wave propagation in beams with periodically attached vibration absorbers: Band-gap behavior and band formation mechanisms". *Journal of Sound and Vibration*, Vol. 332, No. 4, pp. 867–893. ISSN 0022-460X. doi:https://doi.org/10.1016/j.jsv.2012.09.035.

6. RESPONSIBILITY NOTICE

The authors are solely responsible for the printed material included in this paper.